Volume 17, No 4 | International Journal of Radiation Research, October 2019

A fast and accurate analytical method for 2D dose distribution calculation around brachytherapy sources in various tissue equivalent phantoms

R. Bechchar[1], N. Senhou[2], J. ghassoun[1*]

[1]EPRA, Department of Physics, Faculty of Sciences Semlalia, Marrakech, Morocco
[2]Medical Imaging Department, MC 1701, National Guard Health Affairs, King Abdulaziz Medical City, Riyadh, Saudi Arabia

► ***Original article***

Corresponding authors:
J. Ghassoun, PhD.,
Fax: *+ 212 5244 37410*
E-mail: *ghassoun@uca.ac.ma*

Revised: February 2018
Accepted: June 2018

Int. J. Radiat. Res., October 2019; 17(4): 531-540

DOI: 10.18869/acadpub.ijrr.17.3.531

ABSTRACT

Background*:** In this study, a fast dose kernel method (DKM) taking into account an appropriate buildup factor to calculate dose rate distributions around brachytherapy sources was presented. In addition, the dose distribution in various tissue-equivalent materials was investigated using this method. ***Materials and Methods*:** To validate the accuracy of the proposed method, the dose rates in water was calculated by dose kernel method and those obtained by Monte Carlo simulation, thermoluminescent dosimetry (TLD) measurements and AAPM Task Group 43 (TG-43) formalism were compared. The validated dose kernel method (DKM) and the MCNP5 code were then applied to evaluate the effect of tissue composition on dose distribution around a Low Dose Rate (LDR) Ir-192 source located in phantoms simulating water, bone and lung tissue. ***Results: The calculated dose rates were in good agreement with published data for water phantom. Statistical analysis showed that there is no significant difference in terms of dose distribution between the method used in this study and other established methods. Also, the results indicated that the tissue composition affects the dose distribution significantly. Based on the results of this study, the assumption of a homogeneous water phantom in dosimetry of radioactive sources used in brachytherapy may lead to either overestimation of up to 45% or underestimation of up to 19% in bone and lung tissues, respectively. Photon isodose distributions in water, bone and lung were also presented. ***Conclusion:*** Results provides an alternative calculating method for quality assurance purposes using a fast and accurate dose kernel method.

Keywords: *Brachytherapy, Buildup factor, Point kernel, Phantom, Dose, TLD, MCNP.*

INTRODUCTION

Radiation therapy, is a cancer treatment technique that uses ionizing radiation. Brachytherapy is a form of radiotherapy where a radioactive source is placed inside or next to the area requiring treatment. In radiotherapy, accurate dosimetry is essential to achieve local tumor control while avoiding an unacceptable risk to normal tissues. Although standard commercial treatment planning systems (TPS) used in radiotherapy have significantly improved in the last years, they are still limited in terms of estimating dose distributions in heterogeneous media [(1)]. The biological effect of ionizing radiation on human tissues depends on absorbed dose, type of radiation energy and organ irradiated. Photons interacting with body tissues not only lose their energy and finally get absorbed, but also give rise to new photons by multiple scattering. The magnitude of the later effect can be estimated by the so-called buildup

factor.

Several studies have been conducted to examine the dose distributions of Ir-192 wires, using different methods (e.g., film dosimetry or thermoluminesence dosimeter (TLD) measurements, and Monte Carlo simulations, etc.) [2].

In 1995, the American Association of Physicists in Medicine (AAPM) Task Group No. 43 published a protocol including formalism for brachytherapy dose calculation and was later updated in 2004 as TG-43 U1 [3]. This protocol is based on dosimetry parameters such as air-kerma strength (S_K), dose rate constant (Λ), geometry factor $G(r,\theta)$, radial dose function $g(r)$ and anisotropy function. The TG-43 parameters are either measured with suitable detectors or calculated with Monte Carlo simulation techniques [4] and are essential, as they account for accurate determination of dose rate distribution around brachytherapy sources. However, these parameters and the commonly used dose calculation algorithms are based on the assumption of a homogenous water phantom. In clinical cases, the brachytherapy sources are located inside the patient tissues, which are heterogeneous, making the dose very difficult to be assessed accurately [5]. Monte Carlo has been considered as one of the most accurate dose calculation method for determining radiation dose deposition in heterogeneous materials. However, MC simulations have been associated with extremely long calculation time, impeding applications in clinical practice.

In a previous work, Monte Carlo methods were used to determine the effect of tissue inhomogeneities on dose distribution from Cf-252 brachytherapy source [6].

In this study, a simple and fast dose kernel method taking into account an appropriate energy absorption buildup factor (EABF) was developed to calculate dose rate distributions around brachytherapy sources. The buildup factor is a multiplicative factor used to get the corrected response to uncollided photons by including the contribution of scattered photons. It depends on the atomic number of the absorbing medium, the incident energy and the penetration depth, as well as the shape of the radiation source and the medium. To validate the accuracy of our dose kernel method, the dose rates in water phantom obtained by this method were compared with those obtained using Monte Carlo simulation, thermoluminescent dosimeter (TLD) [7] and AAPM TG-43 formalism [8]. The thermoluminescent dosimeters (TLDs) are routinely used to measure the dose around brachytherapy sources due to their small size and high precision [9].

After the *validation,* the dose kernel method and Monte Carlo simulation were used to evaluate the *effect* of *tissue composition* on *dose distribution* around a Low Dose Rate (LDR) Ir-192 brachytherapy source. This effect was evaluated in three *phantoms* consisting of *water*, *bone* and lung *tissue*. In this study, Monte Carlo simulations were performed using the Monte Carlo N-Particle transport code (MCNP5) (X-5, 2003) and $5x10^8$ histories were run to obtain an estimate relative error of less than 1%.

The aim of this study was to use the dose kernel method as a fast and convenient quality assurance method for the verification of dose distributions calculated by the treatment planning system for brachytherapy sources. The choice of this method is motivated by the fact that it takes into account of radiation scattering and attenuation in tissue equivalent phantoms with different compositions.

MATERIALS AND METHODS

Figure 1 shows a schematic diagram of the geometry assumed in the DKM dose calculation around the simulated low dose rate (LDR) Ir-192 brachytherapy source [10]. The source has an effective length of 5 cm and an external diameter of 0.3 mm. The central core was 0.1 mm in diameter encapsulated in a 0.1 mm platinum sheath. We assumed that the radioactive material is uniformly distributed within the Ir-192 core.

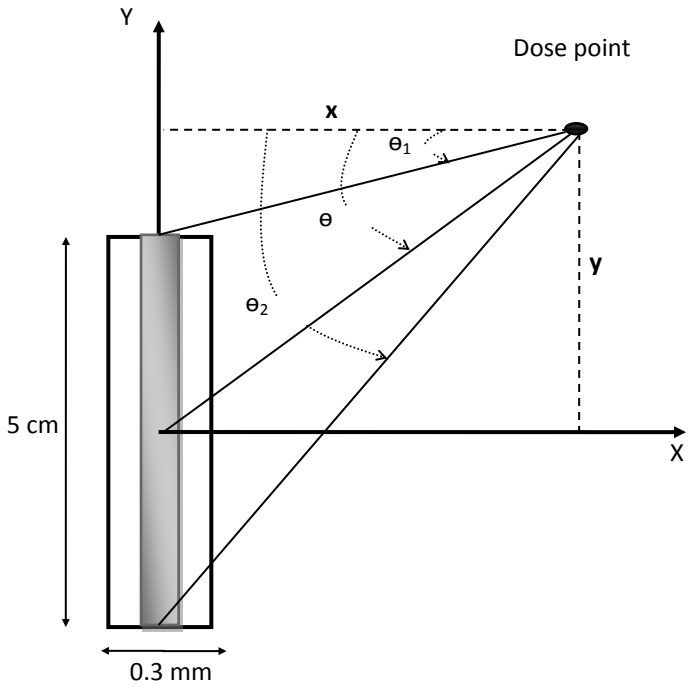

Figure 1. Illustration of the LDR Ir-192 source and the geometry assumed in the dose calculation.

Phantoms

To illustrate the effect of tissue composition on the dose distribution around the simulated LDR Ir-192 brachytherapy source, three spherical phantoms simulating water, bone and lung tissue are used. These phantoms had the same geometric structure but vary in terms of material and density. The elemental compositions and mass densities of these phantoms were adopted from report No. 44 of the International Commission on Radiation Units and Measurements (ICRU) [11]. The mass attenuation coefficients and mass energy absorption coefficients for water, bone and lung tissue were obtained by interpolation of the data published by the National Institute of Standards and Technology (NIST) [12]. The elemental composition and mass densities of the tree phantoms are listed in table 1.

Table 1. The elemental compositions (fraction by weight) and mass density of the three phantoms used in this study.

	H	C	N	O	Na	Mg	P	S	Cl	K	Ca	Density (g/cm$^{3)}$
Cortical bone	0.034	0.155	0.042	0.435	0.001	0.002	0.103	0.003			0.225	1.92
Lung tissue	0.103	0.105	0.031	0.749	0.002		0.002	0.003	0.003	0.002		0.26
Water	0.112	0.888										1.04

Dose kernel method

The absorbed dose rate (Gy/s) at the dose point for a poly-energetic point isotropic photon source is given by equation 1 [13]:

$$\dot{D}(r) = \sum_i A n_i k E_i \left[\frac{\mu_{en}(E_i)}{\rho} \frac{1}{4\pi r^2} e^{-\mu(E_i) r} \right] B_{en}(\mu(E_i) r) \quad (1)$$

where A is the activity of the source in Bq, n_i denotes the number of photon emitted with energy E_i per nuclear disintegration, E_i is the energy emitted by the source in unit of MeV, k is the constant converting energy from the unit of MeV/g to Gy, ρ is the density of the medium in g/cm^3, $\mu(E_i)$ is the linear attenuation coefficient for each energy in cm^{-1}, $\mu_{en}(E_i)$ is the linear absorption coefficient for each energy in cm^{-1} and $B_{en}(\mu(E_i)r)$ is the energy absorption buildup factor. From this formula one can derive the dose rate for a filtered line source.

The dose rate, $d\dot{D}_p$, at point P(x,y) contributed by the source element of length dy is given by the equation 2:

$$d\dot{D}_p = \sum_i S_l n_i k E_i \left[\frac{\mu_{en}(E_i)}{\rho} \frac{1}{4\pi r^2} e^{-\mu(E_i) r} \right] B_{en}(\mu(E_i) r) dy \quad (2)$$

The expression of the elemental dose rate for a point isotropic source given by the equation 2 can be used in determining the dose rate for a line source. As the source density was assumed to be uniformly distributed, the dose rate at point P(x,y) from the centre of the line source is, then, given by equation 3:

$$\dot{D}(x,y) = \int_{-L/2}^{L/2} d\dot{D}_p = \int_{-L/2}^{L/2} \sum_i S_l n_i k E_i \left[\frac{\mu_{en}(E_i)}{\rho} \frac{1}{4\pi r^2} e^{-\mu(E_i) r} \right] B_{en}(\mu(E_i) r) dy \quad (3)$$

Where L is the length of the source and S_l is the linear activity of the source.

The variables r and y may be related to the single variable θ and the fixed perpendicular distance x by the transformations given by equations (4):

$r = x \sec\theta$, $y = x \tan\theta$ and $dy = x \sec^2\theta \, d\theta$ (4)

The integrated dose at point P(x,y) for a line source of length L is then given by equation 5:

$$\dot{D}(x,y) = \sum_i S_l n_i k E_i \int_{\theta_1}^{\theta_2} \left[\frac{\mu_{en}(E_i)}{\rho} \frac{1}{4\pi (x.\sec\theta)^2} e^{-\mu(E_i) x \sec\theta} \right] B_{en}(\mu(E_i) x \sec\theta) x \sec^2\theta \, d\theta \quad (5)$$

Where θ_1 and θ_2 are the angular integration limits. These angles are given by equations 6:

$$\theta_1 = \tan^{-1}\left(\frac{y - \frac{L}{2}}{x}\right) \quad \text{And} \quad \theta_2 = \tan^{-1}\left(\frac{y + \frac{L}{2}}{x}\right) \quad (6)$$

The photon attenuation in the source capsule is taken into account by incorporating an effective attenuation correction using an effective filtration coefficient, μ_b [14]. The expression of dose rate $\dot{D}(x,y)$ in Gy/s at the dose point is then given by equation 7:

$$\dot{D}(x,y) = k \frac{S_l}{4\pi x} \sum_{i=1}^{n} \frac{\mu_{en}(E_i)}{\rho} E_i n_i \int_{\theta_1}^{\theta_2} B_{en}(\mu(E_i) x \sec(\theta)) e^{-(\mu_b(E_i) t + \mu(E_i) x) \sec(\theta)} d\theta \quad (7)$$

where S_l is the linear activity in Bq/cm, $\mu_b(E_i)$ is the effective filtration coefficient in cm^{-1}, t is the capsule thickness in cm.

In this study, the energy absorption buildup factor of water bone and lung tissue was calculated by using the Geometric Progression (G.P) formula given by equations 8 [15]:

$$B(E,r) = 1 + (b-1) r \qquad \text{for} \quad k=1$$

$$B(E,r) = 1 + \frac{(b-1)(K^r - 1)}{K - 1} \qquad \text{for} \quad k \neq 1$$

Where $K(E,r) = cr^a + d \dfrac{\tanh\left(\frac{r}{X_k} - 2\right) - \tanh(-2)}{1 - \tanh(-2)}$

for $r \leq 40$ mfp

where E is the incident energy and r is the distance from the source center in mean free path (mfp). The fitting parameters a, b, c, d and X_k depend on the attenuation medium and source energy. K represents the dose

multiplication factor.

The G.P fitting parameters were determined by the American National Standard Institute (ANSI-6.4.3) [16]. The resulting energy absorption G.P fitting parameters for water, bone and lung tissues were given by S.R Manohara *et al.* [17].

Monte Carlo simulation

The Monte Carlo simulation of radiation therapy treatment allows accurate prediction of the radiation dose distribution delivered to the patient. In this study, the MCNP5 code was used to calculate the dose distribution around an Ir-192 LDR brachytherapy source in water, bone and lung simulating phantoms. The source was placed in the center of spherical phantoms of 15 cm radius and the dose rates were calculated in cells of 2 cm height and 2 cm radius. Moreover, the F8 tally was used for dose calculations. The Ir-192 photon energy spectrum used in this simulation was obtained from Brookhaven National Laboratory [18]. In addition, an apparent activity of 1 mCi/cm was assumed.

Statistical analysis

A statistical analysis of data was performed using IBM SPSS-23 software with an error of α=5%. A p-value less than 0.05 was considered to be statistically significant.

RESULTS

To validate the accuracy of dose kernel method, the dose rates in water phantom determined by this method and those obtained using Monte Carlo simulation, thermoluminescent dosimetry (TLD) measurements and AAPM Task Group 43 (TG-43) formalism were compared.

Table 2 shows a comparison between the measured and the dose kernel method calculated dose rates in water phantom for distances along and away from the source. The dose measurements were carried out using LiF thermoluminescent dosimeter (TLD) chips [7] with dimensions of 1mm × 1 mm × 1mm. The uncertainty in the measurement is approximately ± 4%. In general, a reasonable agreement is obtained. The maximum deviation (D (%)) of 11.18% between measurement and calculation was observed at dose points close to the source (≤ 0.5 cm). In this region, the dose gradient is extremely steep and a measurement device must have both high spatial precision and low sensitivity to rapidly changing radiations dose.

Table 3 shows a comparison of dose rates calculated in water phantom using dose kernel method, MCNP5 code and TG-43 formalism, at different distances along the transverse axis of the source. Dose kernel method calculated results are shown to be in perfect agreement with those obtained using MCNP5 code and TG-43 formalism. The observed maximum percentage difference between the DKM results and the two methods was less than 4.76%.

The t-paired test was used to compare the dose rates calculated by DKM, TLD, MCNP, and TG43 methods. Table 4 shows the p-values of these methods compared with each other.

After the validation, the dose kernel method and the MCNP5 code were used to evaluate the effect of tissue composition on dose distribution around the Ir-192 LDR brachytherapy source. To evaluate the accuracy of the DKM method for dose calculation in different tissue equivalent materials, the dose rates in bone and lung phantoms obtained by this method were compared with those obtained using Monte Carlo simulation. Figure 2 presents the product of dose rate and the square of the distance as a function of distance calculated in bone and lung phantoms using dose kernel method (DKM) and MCNP5 code. As it can be seen, there is a good agreement between the two methods. The maximum percentage difference between the values obtained by the two methods is 4.65% and the maximum mean absolute percentage difference is 2.54% and 1.07% for lung and bone respectively.

Figure 3 shows the relative dose distribution calculated in water, bone and lung phantoms, obtained by dose kernel method, at distances ranging from 0.1 to 15 cm from the source along its transverse axis. The relative dose rate was defined as the ratio of dose rate in bone and lung

to the dose rate in water. From this figure, it can be seen that the tissue elemental compositions have a significant influence on dose distribution especially at distances far from the source. According to the result of the DKM, the percentage difference between the dose rates distribution in water, bone and lung phantoms along transversal axis of the source increases as the distance from the source center increases. Indeed, at depth greater than 5 cm the bone dose would be overestimated by up to 45%, whereas the lung dose would be underestimated by up to 19% at depth greater than 8.5 cm. This behavior is attributed to the differences in mass densities and effective atomic number of these phantoms, which consequently leads to different mass attenuation, absorption coefficient of photons and dose buildup factors.

Table 2. The comparison of dose rates (cGy/h) calculated by dose kernel method (DKM) with thermoluminescent dosimeter (TLD) measurements in water for distances along and away from the source.

Away X(cm)	Along Y(cm)											
	0.0			1.0			2.0			3.0		
	DKM	TLD	D(%)	DKM	TLD	D (%)	DKM	TLD	D(%)	DKM	TLD	D (%)
0.25	54.07	54.10	0.06	53.39	59.80	10.72	48.19	52.30	7.87	7.75	7.00	10.66
0.5	25.32	27.00	6.22	24.68	27.40	9.92	20.70	23.30	11.18	6.45	7.06	8.60
0.75	15.77	15.60	1.11	15.20	15.00	1.36	12.29	12.70	3.19	5.26	5.18	1.62
1.0	11.04	11.00	0.41	10.55	10.90	3.18	8.43	8.94	5.70	4.33	4.36	0.66
1.5	6.41	6.66	3.70	6.07	6.15	1.25	4.90	5.49	10.81	3.08	3.33	7.55
2.0	4.21	4.58	8.14	3.98	3.90	2.08	3.29	3.44	4.45	2.31	2.29	0.73
3.0	2.20	2.26	2.85	2.10	2.25	6.87	1.82	1.91	4.91	1.44	1.47	2.30
4.0	1.33	1.33	0.14	1.28	1.24	3.60	1.15	1.11	4.04	0.97	0.96	1.54
5.0	0.89	0.87	1.79	0.86	0.84	2.55	0.79	0.77	3.16	0.70	0.67	4.25

Table 3. Comparison of dose rates calculated in water phantom, using dose kernel method, MCNP5 code and TG-43 formalism, along the transverse axis of the source.

Distance (cm)	0.25	0.5	1	1.5	2	2.5	3	4	5	6	8	10
MCNP	53.7	25.64	11.34	6.6	4.32	3.05	2.24	1.35	0.89	0.62	0.34	0.21
DKM	54.07	25.32	11.04	6.41	4.21	2.97	2.20	1.33	0.89	0.63	0.35	0.22
$D^{(a)}$(%)	0.71	1.25	2.65	2.88	2.55	2.62	1.79	1.48	0.00	1.61	2.94	4.76
TG43	51.96	24.76	10.98	6.39	4.2	2.96	2.19	1.32	0.87	0.61	0.35	0.22
$D^{(b)}$(%)	4.06	2.26	0.55	0.31	0.24	0.34	0.46	0.76	2.30	3.28	0.00	0.00

Table 4. P-values of the t-paired test resulted from the comparison of DKM, TLD, MCNP and TG43 results.

Compared methods	Distance along the source axis Y(cm)	p-value
DKM-TLD	0.0	0.237
DKM-MCNP	0.0	0.308
DKM-TG43	0.0	0.208
DKM-TLD	1.0	0.195
	2.0	0.088
	3.0	0.978

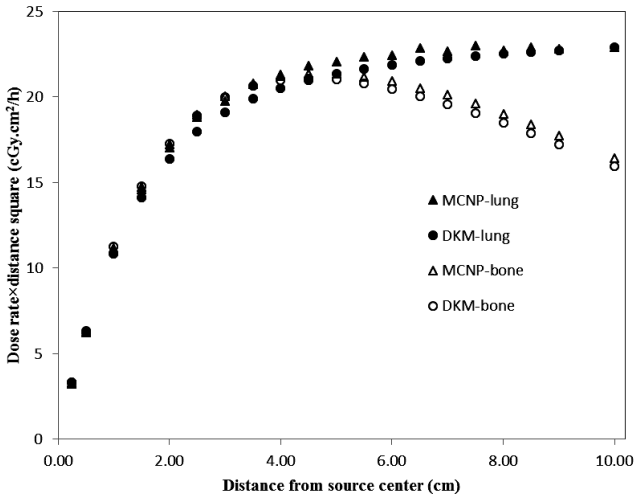

Figure 2. The product of dose rate and the square of the distance as a function of distance calculated in bone and lung phantoms using dose kernel method (DKM) and MCNP5 code.

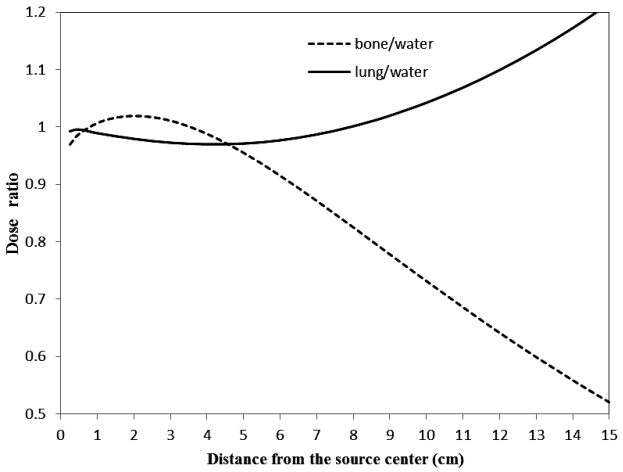

Figure 3. The dose ratio of bone and lung tissue to water calculated using dose kernel method (DKM) along the source transverse axis.

In order to investigate the effect of scattering and attenuation, in each phantom, on the dose distribution around the source, the combined buildup and attenuation factor $B_{en}(\mu x)\exp(-\mu x)$ was evaluated for water, bone, and lung phantoms. This factor was calculated using equation 9 [19]:

$$B_{en}(\mu x)\exp(-\mu x)=\frac{\sum_i n_i E_i B_{en}(\mu(E_i)x)\exp(-\mu(E_i)x)\mu_{en}(E_i)}{\sum_i n_i E_i \mu_{en}(E_i)} \quad (9)$$

Figure 4 shows the variation of the combined buildup and attenuation factor as a function of the distance from the source calculated for water, bone and lung. From this figure, it can be seen that as the distance increased, the combined buildup and attenuation factor decreased much more in bone than in water, and decreased less in lung tissue than in water. Indeed, at distance less than 4 cm from the source, the buildup factor is more than sufficient to compensate for attenuation. However, at distances greater than 4 cm form the source , the compensation for attenuation by scattering is not complete and, therefore, the factor exp(-μx) predominates [20].

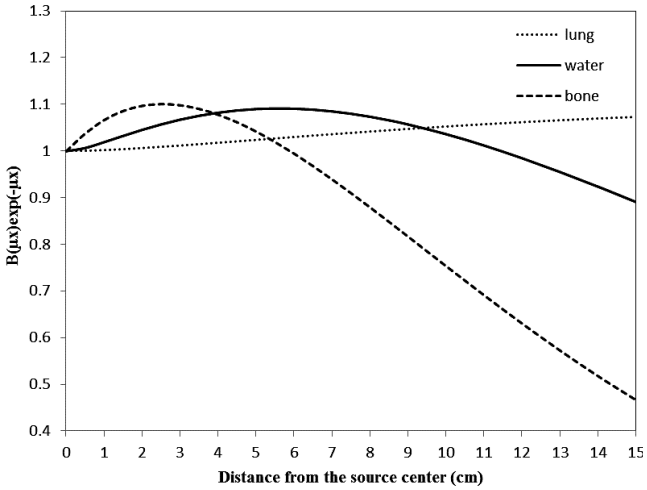

Figure 4. The combined buildup and attenuation factor, Ben(μx)exp(-μx), as a function of distance from the source center at its transverse axis calculated for bone, lung and water.

Figures 5 and 6 show the calculated dose rates using MCNP5 code as a function of energy at distances of 1 and 10 cm, in the lung, bone and water phantoms, respectively. From these figures, it can be seen that the dose rate in bone is higher than that in water and lung tissue especially at lower energies. Furthermore, as the distance from the center of the source increases, the differences between the dose rates in bone, water and lung tissue increase. These differences are due to changes in elemental composition and mass density which confirms the findings stated previously.

Figures 7 and 8 show the DKM calculated two dimensional dose distributions around the source, in the x-y plane, for water–bone and water–lung phantoms, respectively. The isodose curves were normalized to 100% at depth of maximum dose in each phantom. The percentage difference between the dose in water and bone phantoms at transverse plane of the source, increases by increasing the distance from the source center. Moreover, the maximum percentage differences are observed for bone phantoms which confirm the result of Figure 3.

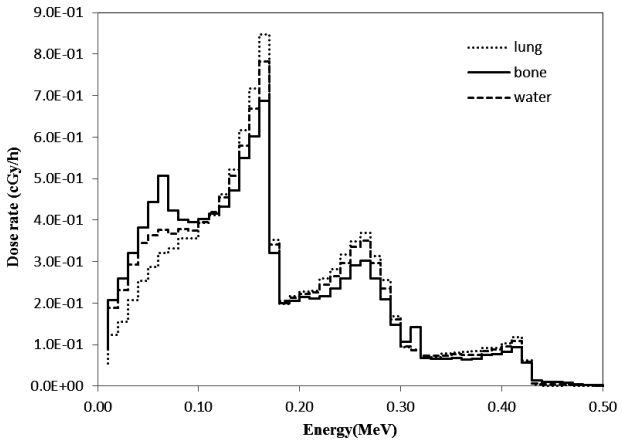

Figure 5. The calculated dose rate as a function of energy in water, bone and lung tissue at a distance of 1 cm from the center of the source along its transverse axis.

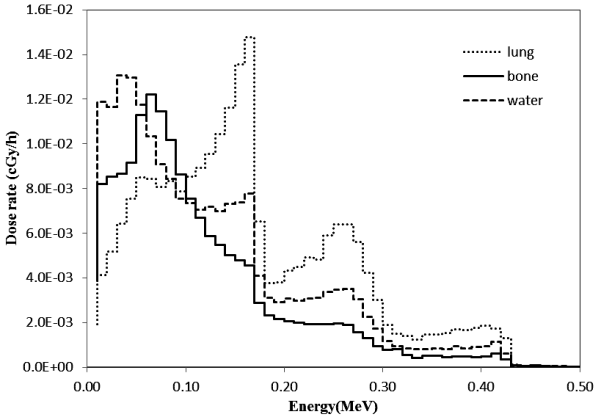

Figure 6. The calculated dose rate as a function of energy in water, bone and lung tissue at a distance of 10 cm from the center of the source along its transverse axis.

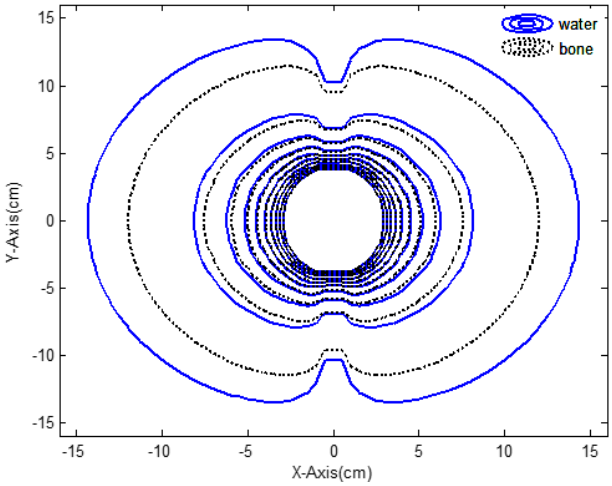

Figure 7. A comparison between the isodose distributions in bone and water.

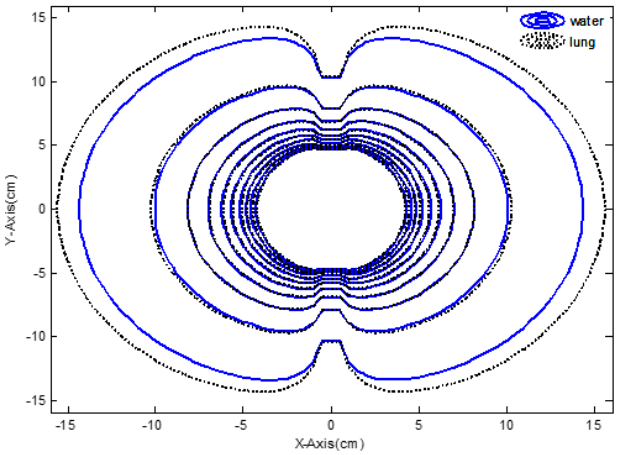

Figure 8. A comparison between the isodose distributions in lung and water.

DISCUSSION

Accurate and fast dose calculation algorithms play an important role in treatment planning because it must be consistent with the dose distribution in the irradiated volume [21].

In this study, a fast and accurate analytical dose kernel method (DKM) taking into account an appropriate energy absorption buildup factor was presented to calculate dose rate distributions around Ir-192 brachytherapy line source. The DKM dose rates calculated in water phantom were validated against experimental measurements performed using thermoluminescent dosimetry (TLD) and also against Monte Carlo simulation results and AAPM TG-34 formalism values (tables 2- 4). A good agreement between the calculated dose rates and published data was obtained. The results of t-paired test indicated that the p-value of any two methods compared with each other is higher than 0.05 which means that there is no significant difference between the calculated dose rates. In addition, the same agreement was observed between DKM and MCNP5 code results in bone and lung phantoms. The small difference observed at distances near the source could mainly due to the interpolation accuracy and also to different cross-section data employed, namely ENDF/B-VI.8 data library in MCNP5 and XCOM/NIST tabulation.

The validated dose kernel method (DKM) and the MCNP5 code are then applied to investigate the effect of tissue *composition* on dose *distribution* around Ir-192 brachytherapy source in three phantoms consisting of water, bone and lung *tissue. This effect increases as the photon energy decreases because of the dependence of photoelectric effect on photon energy and effective atomic number of the absorbing material.* At depth greater than 9 cm the bone dose would be overestimated by up to 45%, whereas the lung dose would be underestimated by up to 19% at depth greater than 8.5 cm. These results are consistent with those obtained by C. H. Wu *et al.* [5] who found an overestimation by 47% at depths greater than 5 cm for bone by using Monte Carlo simulation. Indeed, the tissue elemental compositions and mass densities have a significant influence on dose distribution especially at distances far from the source (figure 2 and 3). This influence can be justified by considering the fact that photoelectric effect has a role in absorption of radiation in tissue. Since bone has a higher effective atomic number due to constituents with higher atomic numbers, the probability of the photoelectric effect in bone is higher than lung and water. As a result, it will receive more doses near the source. On the other hand, the dose decreases much more in bone as the distance increases from the source. These results were in a general agreement with the findings of other workers [20].

According to the combined buildup and attenuation factor $B(\mu x)\exp(-\mu x)$ results (figure 4), it can be seen that as the depth increased, this factor decreased more slowly for lung than for water due to linear attenuation coefficient being small for lung tissue, whereas it decreased faster in bone than in water due to the linear attenuation coefficient being higher in bone than in water. The combined buildup and attenuation factor calculation results agree with the radial dose function simulation results reported by Hsu S-M et al.[20] using EGS4, FLUKA, and MCNP4C codes.

According to the isodose curves (figures 7 and 8), as the distances increased, we found that the dose for lung was higher than water, while the dose for bone was less than water which confirms the findings stated previously. It can also be concluded that the assumption of homogeneous water phantom in dosimetry of radioactive sources, made in brachytherapy, can ultimately leads to either dose overestimation or underestimation in bone and lung tissue respectively. Therefore, tissue composition should be taken into account when accurate dose calculations are required.

CONCLUSION

In this study, a fast dose kernel method (DKM) taking into account an appropriate buildup factor to calculate dose rate distributions around brachytherapy sources was

presented. Dose kernel method calculated results in water phantom are shown to be in perfect agreement with those obtained using MCNP5 code and TG-43 formalism and thermoluminescent dosimetry (TLD) measurements. Statistical analysis of data was performed by IBM SPSS-23 software. The obtained results showed that there is no significant difference between the calculated dose rates in water phantom using the DKM and those obtained using the three methods. In addition, the DKM method was used to evaluate the effect of tissue density and tissue composition on *dose distribution* around the Ir-192 LDR brachytherapy source. The DKM calculated dose rates in bone and lung tissue were compared with those obtained with MCNP5 code. A good agreement was also observed between the two results. In addition, the obtained results showed that the elemental compositions and mass densities, of the tissue equivalent materials, have a significant influence on dose distributions. The results of this study confirmed the accuracy of our DKM for dose calculations around brachytherapy sources.

In this work, we are limited to dose distribution around Ir-192 but dose kernel method which includes the effect of scattering and attenuation in phantoms can further extended to other brachytherapy sources (Pd-103, I-125 and Yb-169) and other tissues such as muscle, fat, brain, etc.

Also, with this method, the effect of tissue heterogeneity can also be taken into account in brachytherapy dose calculation by using two regions buildup factors.

***Conflicts of interest*:** *Declared none.*

REFERENCES

1. Juste B, Miró R, Campayo JM, Díez S, Verdú G (2010) Radiotherapy treatment planning based on Monte Carlo techniques. *Nucl Instr Meth Phys Res A,* ***619 (1)****: 252-257*.
2. Bozkurt A, Acun H, Kemikler G (2013) Dosimetric investigation of LDR brachytherapy 192 Ir wires by Monte Carlo and TPS calculations. *Japanese Journal of Radiology,* ***31(1)****: 24-30*.
3. Rivard MJ, Coursey BM, DeWerd LA, Hanson WF, Kimmel SH, Ibbott GS, Mitch MG, Nath R, Williamson JF (2004) Update of AAPM Task Group No. 43 Report: A revised AAPM protocol for brachytherapy dose calculations. *Med Phys,* ***31(3)****: 633-674*.
4. Zaker N, Zehtabian M, Sina S, Koontz C, Meigooni1 AS (2016) Comparison of TG-43 dosimetric parameters of brachytherapy sources obtained by three different versions of MCNP codes. *J Appl Clin Med Phys,* ***17(2)****: 379-390*.
5. Wu CH, Liao YJ, Liu YW, Hung SK, Lee MS, Hsu SM (2014) Dose distributions of an Ir-192 brachytherapy source in different media. *BioMed Res Int, 2014: 946213*.
6. Ghassoun J (2013) Effect of tissue Inhomogeneities on dose distributions from Cf-252 brachytherapy source. *Appl Radiat Isot,* ***71(1)****: 1-6*.
7. Gillin MT, Lopez F, Kline RW, Grimm DF, Niroomand-Rad A (1988) Comparison of measured and calculated dose distributions around an iridium 192 wire. *J Med Phys,* ***15 (6)****: 915-918*.
8. Van der Laarse R, Granero D, Pérez-Calatayud J, Meigooni A, Ballester F (2008) Dosimetric characterization of Ir-192 LDR elongated sources. *Med Phys,* ***35(3)****: 1154-1161*.
9. DeWerd LA, Liang Q, Reed JL, Culberson WS (2014) The use of TLDs for brachytherapy dosimetry. *Radiation Measurements,* ***71****: 276-281*.
10. Karaiskos P, Papagiannis P, Angelopoulos A, Sakelliou L (2000) Dosimetry of Ir-192 wires for LDR interstitial brachytherapy following the AAPM TG-43 dosimetric formalism. *Med Phys,* ***28(2)****: 156-166*.
11. International Commission on Radiation Units and Measurements (1989) Tissue substitutes in radiation dosimetry and measurement. *ICRU Report no. 44, Bethesda*.
12. Hubbell JH and Seltzer SM (1995) Tables of X-ray mass attenuation coefficients and mass energy-absorption coefficients 1 keV to 20 MeV for elements Z= 1 to 92 and 48 additional substances of dosimetric interest, NISTIR 5632, National Institute of Standards and Technology.
13. Chen Z and Nath R (2001) Dose rate constant and energy spectrum of interstitial brachytherapy sources. *Med Phys,* ***28(1)****: 86-96*.
14. Sakhri-Brahimi Z, Guedioura D, Khelassi-Toutaoui N, Afiane M, Frahi-Amroun A (2018) Reference kerma rate evaluation using Sievert integral for extended sources. In AIP Conference Proceedings. *AIP Publishing,* ***1994(1)****: 060005*.
15. Harima Y, Sakamoto Y, Tanaka S, Kawai M (1986) Validity of the geometric-progression formula in approximating gamma-ray buildup factors. *Nucl Sci Eng,* ***94(1)****: 24-35*.
16. ANSI/ANS-6.4.3 (1991) Gamma Ray Attenuation Coefficient and Buildup Factors for Engineering Materials. American Nuclear Society, La Grange Park, Illinois.
17. Manohara SR, Hanagodimath SM, Gerward L (2011) Energy absorption buildup factors of human organs and tissues at energies and penetration depths relevant for radiotherapy and diagnostics. *J Appl Clin Med Phys,* ***12(4)****: 296-312*.
18. Tuli JK (1987) Evaluated Nuclear Structure Data File. Brookhaven National Laboratory Nuclear Data Center.
19. Angelopoulos A, Perris A, Sakellariou K, Sakelliou L, Sarigiannis K, Zarris G (1991) Accurate Monte Carlo calculations of the combined attenuation and build-up factors for energies (20-1500 keV) and distances (0-10 cm) relevant in brachytherapy. *Phys Med Biol,* ***36****: 763–778*.
20. Hsu SM, Wu CH, Lee JH, Hsieh YJ, Yu CY, Liao YJ, Huang DY (2012) A study on the dose distributions in various materials from an Ir-192 HDR brachytherapy source. *PloS one,* ***7(9)****: e44528*.
21. Kim YL, Suh TS, Choe BY, Choi BO, Chung JB, Lee JW, Kim JY (2016) Dose distribution evaluation of various dose calculation algorithms in inhomogeneous media. *Int J Radiat Res,* ***14(4)****:269*.